RESEARCH ARTICLE | JANUARY 11 2007

Highly efficient near-infrared organic excimer electrophosphorescent diodes

M. Cocchi; D. Virgili; V. Fattori; J. A. G. Williams; J. Kalinowski

Appl. Phys. Lett. 90, 023506 (2007)
https://doi.org/10.1063/1.2430926

Highly efficient near-infrared organic excimer electrophosphorescent diodes

M. Cocchi,[a] D. Virgili, and V. Fattori
Institute of Organic Synthesis and Photoreactivity, National Research Council of Italy (ISOF-CNR), I-40129 Bologna, Italy

J. A. G. Williams
Department of Chemistry, University of Durham, Durham DH1 3LE, United Kingdom

J. Kalinowski[b]
Department of Molecular Physics, Gdańsk University of Technology, 80-952 Gdańsk, Poland

(Received 18 October 2006; accepted 5 December 2006; published online 11 January 2007)

The authors report the fabrication of very high efficiency near-infrared (NIR) organic light-emitting diodes (LEDs) based on a series of terdentate cyclometallated phosphorescent Pt(II) complexes Pt*L*Cl as the emitting layer. The LEDs exhibit exclusive NIR excimeric phosphorescence peaking between 705 and 720 nm for three different organic ligands (*L*). Due to the high excimer emission quantum yields of these Pt complexes and to confinement of the recombination zone within the emission layer, unusually high external quantum efficiencies from 9.8% to 10.7% photons/electron and a high forward light output exceeding 15 mW/cm^2 were achieved. © *2007 American Institute of Physics*. [DOI: 10.1063/1.2430926]

The development of organic light-emitting diodes (LEDs), based on sublimed small molecules, has proceeded rapidly since the initial work by Tang and VanSlyke.[1] Due to promising prospects for next generation of lighting and display technology, most efforts have been directed towards light emission in the visible range.[2] However, other applications, e.g., in communications or biomedicine, call for optoelectronic devices operating in the near-infrared (NIR) spectral range. Various approaches have been explored for obtaining infrared emission from organic LEDs. The use of rare earth complexes and small optical gap polymers has been attracting interest since lanthanide ions such as Er^{3+} or Nd^{3+} reveal NIR emission,[3,4] and the polymer emission extends to a wavelength of 1000 nm.[5] One of the most important shortcomings of the NIR LEDs is poor quantum efficiency and low power output. For example, a forward light output of 100 μW/cm^2 and only 0.1% of external quantum efficiency have recently been reported for NIR electrophosphorescence with a peak value at 720 nm from blends of polymeric host and an iridium (III) organic complex.[6] A dispersion of inorganic indium arsenide-based nanocrystals in conjugated polymers has been employed to improve the quantum efficiency by not more than ≈0.5% photon/electron.[7]

In this work, we have fabricated highly efficient (>10% photon/electron) organic electroluminescent devices using neat film emitters made of terdentate cyclometallated phosphorescent Pt(II) complexes PtL^nCl which exhibit exclusive NIR excimer emission peaking at wavelengths between 705 and 720 nm for different ligands, L^n (n=1,2,3). The synthesis of PtL^nCl has been described previously.[8] The LED structure and materials used along with their energy level positions are shown in Fig. 1. Commercially available indium tin oxide (ITO) with a sheet resistivity of 20 Ω/sq on glass substrates was used in the device fabrication process. In the device architecture two hole- and exciton-blocking layers (CBP and OXA) were introduced to confine the electron-hole recombination and emission processes within the emitting layer of neat PtL^nCl emitters. A 70 nm thick hole-transporting layer of [*N*,*N*′-bis (3-methyl)-1,1′-biphenyl-4,4′ diamine (TPD)]:[bisphenolpol-A-polycarbonate (MW 32000-36000) (PC)] (Aldrich and Polysciences Inc., respectively) blend was spun on top of the ITO from a 10 mg/ml dichloromethane solution at room temperature. It was followed by a vacuum evaporated 20 nm thick hole-blocking layer of 4,4′-*N*,*N*′-dicarbazole-biphenyl (CBP). The active emissive layers of the three Pt complexes reported in Fig. 1 were evaporated under a vacuum of 10^{-5} hPa on top of the CBP layer. Subsequently evaporated on them was a 30 nm thick layer of 3,5-bis[5-(4-tert-butylphenyl)-1,3,4-oxadiazol-2-yl]-benzene (OXA) (Syntech) which served as an electron transporting, and hole- and exciton-blocking layer. Each layer thickness was measured with a Tencor Alpha Step 200 profilometer. The opposing electrodes of calcium, used to inject electrons, were deposited on the electron transporting layer of OXA by thermal evaporation *in vacuo*. The highest occupied molecular orbital (HOMO) levels of all the compounds were estimated from their oxidation potentials. The oxidation potentials were determined by cyclic voltammetry using the standard calomel electrode (SCE) in $10^{-3}M$ dichlo-

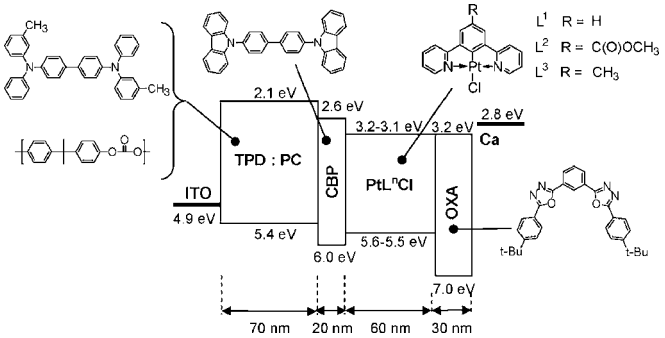

FIG. 1. Energy level diagram of the EL devices and molecular structures of the materials used. For chemical names of the materials see text.

[a]Electronic mail: cocchi@isof.cnr.it
[b]Electronic mail: kalino@polnet.cc

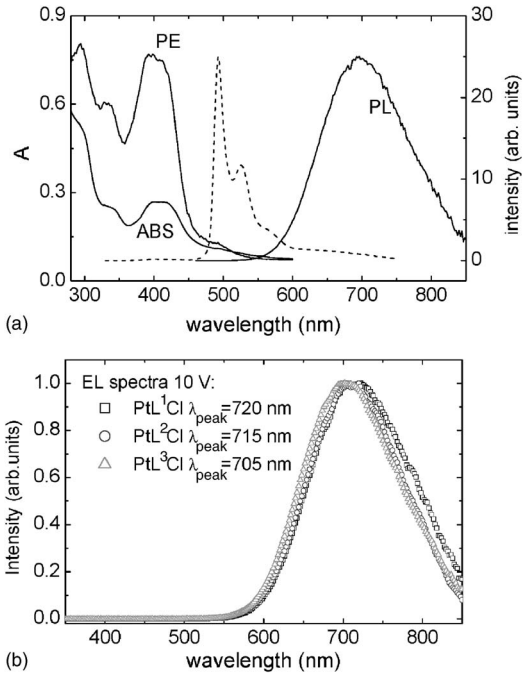

FIG. 2. (a) Absorption (ABS), photoluminescence (PL) at $\lambda_{exc}=350$ nm, and photoexcitation at $\lambda=650$ nm spectra of a 60 nm thick neat PtL^1Cl film. The PL spectrum of a polycarbonate film containing 6 wt % of PtL^1Cl is displayed for comparison (dashed line). (b) Electroluminescence spectra recorded at the applied voltage of 10 V for devices presented in Fig. 1. The peak positions of the spectra are given in the left-upper corner of the figure.

romethane solutions for TPD, OXA, and CBP. For all of these three compounds fully reversible oxidation waves have been observed with a scan speed 100 mV/s. The lowest unoccupied molecular orbital (LUMO) levels were estimated from ionization potentials and electronic absorption bands. Their values are within ±0.1 eV in agreement with those reported previously for TPD (Ref. 9) and CBP.[10] The oxidation potentials of the complexes were determined using the SCE in $10^{-3}M$ acetonitrile solutions. In all cases irreversible oxidation waves have been observed with a scan speed 300 mV/s. Electrochemical data for the reduction potential of PtL^nCl ($E_p^{red}=-1.93$ V vs Fc^+/Fc) (Ref. 11) locate its LUMO at 3.17 eV below the vacuum level. Device characterization was carried out in argon atmosphere at room temperature. The spectral characteristics of the materials and devices under study were measured with a Perkin-Elmer Lambda 19UV/VIS/NIR spectrometer and a StellarNet spectroradiometer, and a single-photon IBH model 5000 counter was employed for the time resolved luminescence measurements. The current-voltage characteristics of the devices were measured with a Keithley source measure unit model 236, under continuous operation mode, while the light output power was measured with an EG&G power meter.

Figure 2 compares the photoluminescence (PL) and electroluminescence (EL) spectra of neat PtL^nCl emitters ($n=1,2,3$) displayed along with their absorption and photoexcitation spectra. A 100% pure film of PtL^1Cl, representative of the behavior of all PtL^nCl complexes in solid state, shows only a broad featureless PL band extending from 620 to 760 nm with a full width at half maximum of 140 nm and peak at about 680 nm [Fig. 2(a)]. The infrared portion (above 750 nm) constitutes about 40% of the total emission output. On the other hand, the emission of PtL^1Cl obtained at low concentration (6 wt %) in a polycarbonate matrix shows

TABLE I. Photophysical properties (all measurements were carried out in argon atmosphere at room temperature) of the studied Pt complexes in neat solid films.

Pt complex (60 nm thick films)	τ_0 (μs)[a] (±0.05 μs)	η_{PL}[b] (±0.07)	HOMO (eV)[c]	LUMO (eV)[c]
PtL^1Cl	0.98	0.24	5.53	3.07
PtL^2Cl	1.07	0.35	5.57	3.17
PtL^3Cl	1.10	0.31	5.47	3.08

[a]The excimer lifetime τ_0 obtained from fit to the monoexponential decay of PL.
[b]Calculated using standard BASF LumogenF Red 300.
[c]Derived from redox potentials (Ref. 12).

a structured blueshifted spectrum characteristic of molecular phosphorescence observed in solutions.[8,11] The absence of the molecular phosphorescence in the emission spectra of neat films suggests the bimolecular-based weakly bound dimer or excimer excited states to be responsible for their broad band structureless emission spectra. The photoexcitation spectrum, shown in Fig. 2(a), provides evidence of direct sensitization of the excimerlike emission via the $^3\pi$-π^* excited state of the single molecule. The absorption and excitation spectra in the film are not significantly different from those in solution, and there is no compelling evidence for the presence of ground-state aggregates or dimers. The PL quantum efficiency (η_{PL}) and excimer lifetimes along with HOMO and LUMO levels for all three complexes under study are summarized in Table I.

While the absorption is underlain by monomolecular electronic transitions, the PL [Fig. 2(a)] and EL [Fig. 2(b)] of neat PtL^nCl films exhibit bimolecular-based excimer radiative relaxation. No monomolecular phosphorescence is observed due to the efficient formation of excimers under both optical (PL) and electrical (EL) excitations of the neat vacuum-evaporated Pt complex films studied. Like phosphorescent molecules of the cyclometallated complex of platinum (II) (2-(4′,6′-difluorophenyl)pyridinato-N,C^2)acetyl acetate (FPt1), molecules of PtL^nCl have a planar structure, facilitating formation of triplet excimers.[13] The triplet character of the excimer state is confirmed by the luminescent decay which, like that for FPt1,[13] shows measured lifetimes about 1 μs. Exclusive NIR emission with peaks of 705 nm (PtL^3Cl), 715 nm (PtL^2Cl), and 720 nm (PtL^1Cl) is observed for EL, corresponding to the Commission Internationale de L'Eclairage coordinates of $x\approx0.68$ and $y\approx0.31$.

The EL and PL spectra of the neat films are shifted by about 40 nm [cf. Figs. 2(a) and 2(b) for PtL^1Cl]. We assign this shift to the different contributions of the charge-transfer (CT) resonance component of the overall triplet excimer state described by a function[2]

$$^3|M_1M_2\rangle^* = c_1\ ^3|M_1M_2\rangle^*_{EX} + c_2\ ^3|M_1M_2\rangle^*_{CT}, \quad (1)$$

expressing the quantum mechanical mixing of the excimer formed by the exciton resonance (EX) interaction, $^3|M_1M_2\rangle^*_{EX}=a_1\ ^3|M_1^*M_2\rangle+a_2\ ^3|M_1M_2^*\rangle$, and that resulting from the CT resonance interaction, $^3|M_1M_2\rangle^*_{CT}=b_1\ ^3|M_1^+M_2^-\rangle+b_2\ ^3|M_1^-M_2^+\rangle$, between two molecules (M_1,M_2) of the emissive material. Whereas the coefficients c_1 and c_2 determine the contributions of the EX and CT interaction components to the excimer, the coefficients a_1 and a_2 are the amplitudes of the two component state of the EX configuration emerging as a result of the excitonic reso-

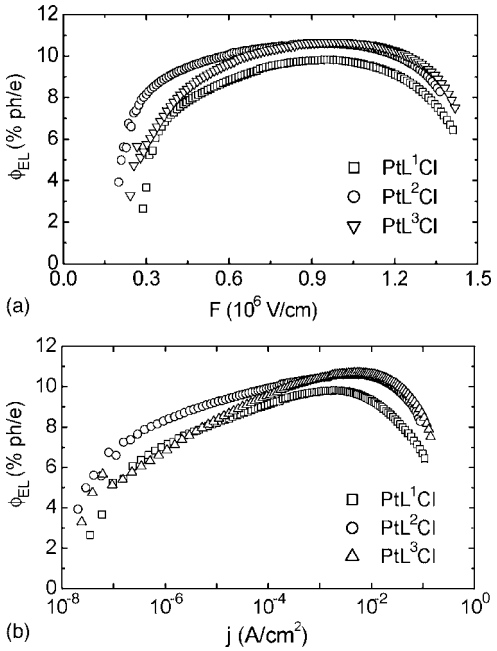

FIG. 3. External EL quantum efficiency $[\varphi_{EL}^{(ext)}]$ vs applied field (a) and driving current density (b) for devices described in Fig. 1. The Lambertian angular distribution of the emission has been assumed in the calculation of $\varphi_{EL}^{(ext)}$.

nance between states $^3|M_1^*M_2\rangle$ and $^3|M_1M_2^*\rangle$ with the excitation localized either on the molecule M_1 or on molecule M_2, respectively. Furthermore, the coefficients b_1 and b_2 determine the amplitudes of two extreme CT states, $^3|M_1^+M_2^-\rangle$ and $^3|M_1^-M_2^+\rangle$. The relation between amplitudes of function (1) and thus the excimer energy depends on the distance between molecules M_1 and M_2 and their mutual orientation. The states with a negative CT resonance energy component have the lowest energies.[2] The direct electron-hole recombination mechanism of the excimer formation favors the low-energy CT states to dominate the excimer character (1), observed as a redshift in the EL emission spectrum.

The maximum room temperature external quantum efficiency of the devices in Fig. 1 is $\varphi_{EL}=(10.5\pm0.5)\%$ photons/electron at a current density 10 mA/cm^2 or an electric field 10^6 V/cm (Fig. 3). It is nearly quadruple the efficiency reported for the triplet excimer red ($\approx$600 nm) emission from an organic LED based on another Pt(II) complex FPt1,[13] and as much as 100 times larger than that from an organic LED based on molecular electrophosphorescent complex of Ir(III),[6] emitting in the NIR (720 nm) region of the electromagnetic wave spectrum. Even at low current densities (down to 10^{-4} mA/cm^2), the φ_{EL} exceeds these figures by 2 and 60 times, respectively, as seen in Fig. 3(b). A high forward light output reaching 15.9 mW/cm^2 has been detected at $\sim$100 mA/cm^2 with $\varphi_{EL}=8.5\%$ photons/electron and luminous efficiency=5.5 cd/A for PtL^3Cl.

The field (current density) dependence of the external quantum yield displayed in Fig. 3 can be understood in terms of the field-dependent optical external coupling (ξ), width of the recombination zone (w), and the emission efficiency of the excited species $[\varphi_r(F)\rightarrow\eta_{PL}$ for $F\rightarrow 0]$,[2]

$$\varphi_{EL}^{(ext)}=\xi P_T\varphi_r(1+w/d_e)^{-1}, \quad (2)$$

where $P_T\approx 1$ is the probability of producing a triplet excimer, and d_e is the thickness of the emitter layer. The increasing field imposes narrowing and shifting of the recombination zone towards the strongly hole-blocking layer of OXA (cf. Fig. 1). A similar effect has been observed earlier with classical bilayer Alq_3-based LEDs.[14] The concomitant increase of the light output coupling factor ξ is expected as the narrowing near-OXA region recombination zone moves "the center of gravity" of the emissive species away from the air/ITO glass interface forming side waveguiding modes responsible for light losses in the photon flux detected perpendicular to the planar cell through the ITO anode.[15] While both of them lead to a field increasing apparent quantum efficiency, the field decrease in φ_r (F), caused by the field-assisted dissociation, and quenching of excited states by the injected charge lead to a reduction of $\varphi_{EL}^{(ext)}$,[16] the latter being a dominating factor at high electric fields. As a result a nonmonotonic behavior of the external EL efficiency with electric field is observed.

In conclusion, we have fabricated a series of devices utilizing terdentate cyclometallated Pt(II) complexes as emitters. Their solid state neat films have excellent characteristics coupled to highly efficient exclusive NIR excimer emission, demonstrating that the efficient excimer phosphorescence can be used to fabricate highly efficient NIR excimer electrophosphorescent diodes.

This work was supported by the Italian CNR Project No. PM.P04.004.002, MIUR-FIRB Project No. RBNE019H9K, and by the European COST Project No. D35-0010-05.

[1] C. W. Tang and S. A. VanSlyke, Appl. Phys. Lett. **51**, 913 (1987).
[2] J. Kalinowski, *Organic Light Emitting Diodes: Principles, Characteristics, and Processes* (Dekker, New York, 2005).
[3] R. G. Sun, Y. Z. Wang, Q. B. Zheng, H. J. Zhang, and A. J. Epstein, J. Appl. Phys. **87**, 7589 (2000).
[4] O. M. Khreis, R. J. Curry, M. Somerton, and W. P. Gillin, J. Appl. Phys. **88**, 777 (2000).
[5] D. R. Baigent, P. J. Hamer, R. H. Friend, S. C. Moratti, and A. B. Holmes, Synth. Met. **71**, 2175 (1995).
[6] E. L. Williams, J. Li, and G. E. Jabbour, Appl. Phys. Lett. **89**, 083506 (2006).
[7] N. Tessler, V. Medvedev, M. Kazes, S. H. Kan, and U. Banin, Science **295**, 1506 (2002).
[8] J. A. G. Williams, A. Beeby, E. S. Davis, J. A. Weinstein, and C. Wilson, Inorg. Chem. **42**, 8609 (2003).
[9] H. Ogawa, R. Okuda, and Y. Shirota, Appl. Phys. A: Mater. Sci. Process. **67**, 599 (1998).
[10] M. A. Baldo and S. R. Forrest, Phys. Rev. B **62**, 10958 (2000).
[11] M. Cocchi, D. Virgili, V. Fattori, D. L. Rochester, and J. A. G. Williams, Adv. Funct. Mater. (in press).
[12] S. J. Farley, D. L. Rochester, A. L. Thompson, J. A. K. Howard, and J. A. G. Williams, Inorg. Chem. **44**, 9690 (2005).
[13] B. D'Andrade and S. R. Forrest, Chem. Phys. **286**, 321 (2003).
[14] J. Kalinowski, L. C. Palilis, W. H. Kim, and Z. H. Kafafi, J. Appl. Phys. **94**, 7764 (2003).
[15] V. Bulović, V. B. Khalfin, G. Gu, P. E. Burrows, D. Z. Garbuzov, and S. R. Forrest, Phys. Rev. B **58**, 3730 (1998).
[16] J. Kalinowski, W. Stampor, J. Szmytkowski, D. Virgili, M. Cocchi, V. Fattori, and C. Sabatini, Phys. Rev. B **74**, 085316 (2006).